Experimental study of fish-friendly angled bar racks with horizontal bars

Fatma Lemkecher, Ludovic Chatellier, Dominique Courret, Laurent David

Research paper

Experimental study of fish-friendly angled bar racks with horizontal bars

FATMA LEMKECHER, PhD Student, *Institut Pprime, CNRS—Université de Poitiers—ENSMA, Pôle R & D écohydraulique OFB-IMFT-PPRIME, UPR 3346, 11 Boulevard Marie et Pierre Curie, Site du futuroscope, 86073 Poitiers, France.*
Email: fatma.lemkecher@univ-poitiers.fr (author for correspondence)

LUDOVIC CHATELLIER, Assistant Professor, *Institut Pprime, CNRS—Université de Poitiers—ENSMA, Pôle R & D écohydraulique OFB-IMFT-PPRIME, UPR 3346, 11 Boulevard Marie et Pierre Curie, Site du futuroscope, 86073 Poitiers, France.*
Email: ludovic.chatellier@univ-poitiers.fr

DOMINIQUE COURRET, Environmental Engineer, *Office Français de la Biodiversité – DRAS, Pôle R & D écohydraulique OFB-IMFT-PPRIME, 2 Allée du Professeur Camille Soula, 31400 Toulouse, France.*
Email: dominique.courret@imft.fr

LAURENT DAVID (IAHR Member), Professor, *Institut Pprime, CNRS—Université de Poitiers—ENSMA, Pôle R & D écohydraulique OFB-IMFT-PPRIME, UPR 3346, 11 Boulevard Marie et Pierre Curie, Site du futuroscope, 86073 Poitiers, France.*
Email: laurent.david@univ-poitiers.fr

ABSTRACT
This paper presents an experimental study of angled fish-friendly bar racks with horizontal bars, using a physical model in an open channel. Head losses are investigated for two bar shapes, three ratios between bar spacing and bar thickness and four angles of orientation of the racks. The Froude and bar-Reynolds numbers were respectively 0.275 and 3600. The head loss coefficients decrease as the blockage ratio and the angle of orientation of the rack decrease. They are well predicted by a formula produced previously for an inclined rack, with some adaptations. Velocity fields are characterized upstream and downstream of the racks, showing no effect of the angle of orientation and no heterogeneity over channel width. Consequently, the normal and tangential components of the velocity along the rack are in agreement with the theoretical values given by angular decomposition. These results serve to assess the compliance with biological criteria to avoid impingement risks and guide fish towards a bypass.

Keywords: Angled trash racks; fish-friendly; horizontal bars; downstream fish migration; head losses; velocity profiles

1 Introduction

Hydropower plants represent almost a sixth of the world-wide electricity production (IEA, 2017), and its development as a renewable energy is promoted in Europe by Directive 2009/28/CE (2009). However, the multiplication of hydroelectric power plants along fish migration routes may lead to important cumulative impacts on several endangered migratory species, such as salmon, sea trout and eels, notably during their downstream migration (Electric Power Research Institute, 2001; Huusko et al., 2018; Larinier & Travade, 2002; Montén, 1985; Verbiest et al., 2012).

In Europe, restoring the longitudinal connectivity of rivers, including downstream migration, is increasingly addressed as part of plans for renewal or conservation of migratory species, and to sustain the acceptable ecological status of rivers according to the European Water Framework Directive (2000/60/EC). In addition, European Council regulation no. 1100/2007 established measures for the recovery of European eel stocks. This includes the requirement that all member states reduce anthropogenic mortality factors and in particular injuries inflicted on silver eels migrating downstream when they pass through turbines.

The installation of fish-friendly intakes, combining low bar-spacing rack set-ups and bypasses, is one of the most frequently implemented solutions at small to medium HPPs (turbine discharge of up to $100\,m^3\,s^{-1}$) (Courret et al., 2015). To be considered as fish-friendly, bar racks must have small clear spaces between their bars to avoid the passage of fish through the turbines (less than 25 mm for salmon and sea trout smolts and less

than 15–20 mm for silver eels). These racks have a behavioural effect on small fishes (juveniles) and constitute a physical barrier for large ones (adults). The bar racks should be inclined or angled to guide fish toward the bypasses located at the downstream end of the racks (Courret & Larinier, 2008; Courret et al., 2015). To avoid impingement of smolts and silver eels on a rack, it is recommended that the normal velocity should not exceed 0.5 m s^{-1}. In the case of angled racks, to efficiently guide fish to the downstream end of the rack towards the bypass entrance, it is recommended that the ratio between the tangential and the normal velocities is equal to or higher than 1.

Low bar-spacing racks can generate high head losses that constitute energy losses for hydroelectric operators. Velocity heterogeneity downstream of racks can also be an issue if the turbine intake is near to the rack (Godde, 1994).

Concerning angled racks, several studies have focused on head losses and velocity fields, since the 1920s (reviewed in Albayrak et al., 2018; Raynal et al., 2013b). Classical angled racks, composed of vertical bars perpendicular to the rack axis, and so angled to the flow direction, have several disadvantages as they generate high amounts of head losses and heterogeneous flow fields upstream and downstream of the rack (Albayrak et al., 2018; Amaral et al., 2003; Raynal et al., 2013b). This limits their applicability at hydropower plant intakes.

Modified angled racks with vertical bars in a streamwise position studied by Raynal et al. (2014) generate lower head losses. The rack orientation then has no influence, and the uniformity of the flow fields is improved. However, to our knowledge, there is still no full-scale installation of such racks at intakes of hydropower plants.

Angled racks with horizontal bars also appear to be a new solution. This configuration emerged recently in Germany and has already been implemented at several intakes with discharge of up to 88 m^3 s^{-1} (Ebel, 2013). However, head losses and flow fields upstream and downstream of such racks are still rarely studied, with only a few papers having recently been published for a limited number of configurations (Albayrak et al., 2020; Böttcher et al., 2019).

The current experimental study on angled racks with horizontal bars aims to investigate wide ranges and many combinations of rack angles, bar shapes and ratios between bar spacing and bar thickness. The objective is to produce a formula to assess head losses and to characterize upstream and downstream flow fields. Section 2 describes the experimental set-up and presents the main characteristics of the hydraulic installation, the bar rack model and the different measurement devices. Section 3 focuses on head losses and presents the experimental results in comparison with previous studies and formulae. The applicability of the formula proposed by Raynal et al. (2013a) for inclined racks is investigated. A comparison of the head loss coefficients for several types of angled racks is also carried out. Section 4 analyses the velocity profiles and their compliance with biological criteria. Furthermore, a comparison of velocity profiles for several types of angled racks is conducted. These results are then discussed in Section 5 with recommendations for the design of fish-friendly water intakes.

2 Experimental set-up

The experiments were conducted in a 1 m wide, 1 m deep and 12 m long open channel at the Institut Pprime, with a PVC bed and glass side walls (1). A weir at the outlet of the flume serves to adjust the water head. The flow rate (Q) of 1800 m^3 h^{-1} (0.5 m^3 s^{-1}) and the water depth (H_1) of 0.7 m were maintained for an approach velocity (V_1) of 0.72 m s^{-1} after investigating two discharges of 0.375 and 0.5 m^3 s^{-1} to verify the invariance with respect to the Reynolds and Froude numbers. According to previous studies (Albayrak et al., 2018; Raynal et al., 2013a), the head loss coefficient is invariable for a Reynolds number higher than 3000 and for a Froude number F higher than 0.1. In our experiments, the Froude number was about 0.275 and the bar-Reynolds number ($R_{eb} = \rho \times b \times V_1/\mu$) was 3600 for the flow rate of 0.5 m^3 s^{-1}.

The bar racks (2 and 3) were composed of three principle components: the bars, the spacers and the support elements. Bar thickness and depth are noted (b) and (p) respectively. Two bar profiles were tested: rectangular (PR) and hydrodynamic (PH) that has a rounded front edge and a tapered back edge, used in the previous study of Raynal et al. (2013a). The rack was oriented at four angles (α): 30°, 45°, 60° and 90° (4). For each angle and bar profile, three bar spacings (e) were tested: 5, 10 and 20 mm. These correspond to (e/b) ratios equal to 1, 2 and 4, respectively. All the parameters are summarized in Table 1. The model scale 1:2 refers to the bar width, thickness and spacing generally used in the real sites.

The water depth measurements were carried out with four water surface gauges (5). These gauges were ultrasonic from

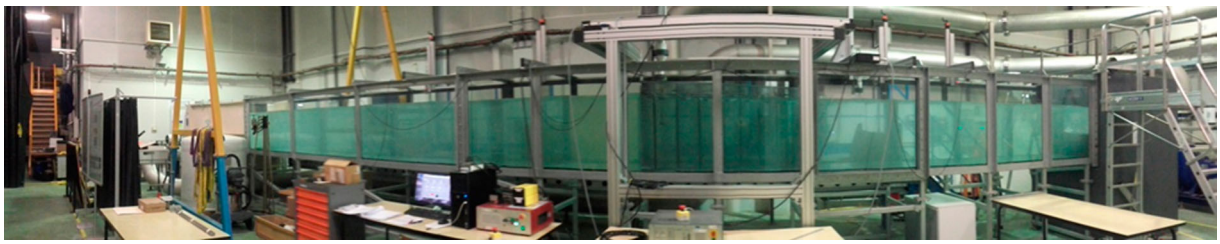

Figure 1 Open flow channel at the Pprime institute

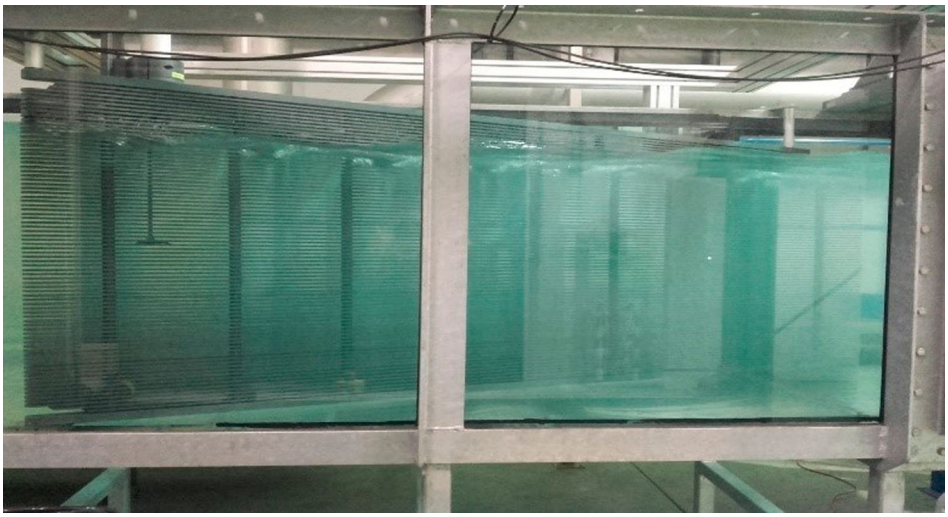

Figure 2 Angled trash rack with horizontal bars

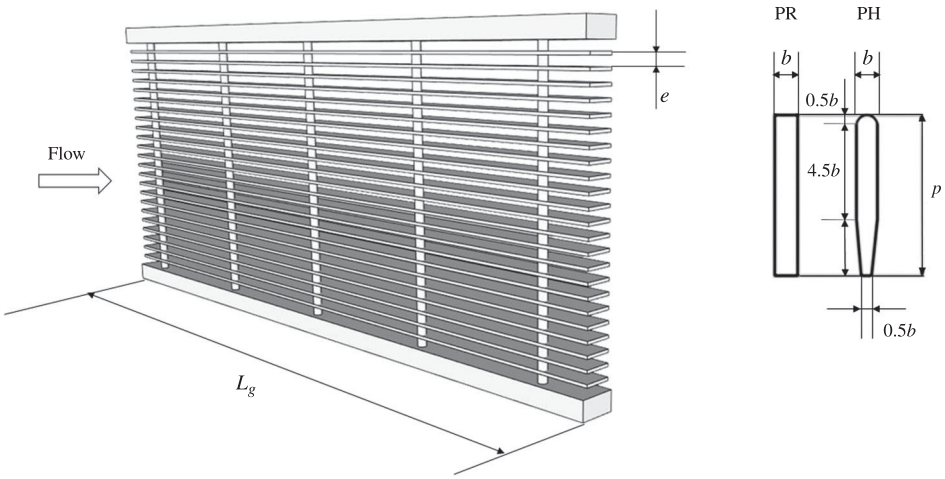

Figure 3 Trash rack with parameters and different types of bar section

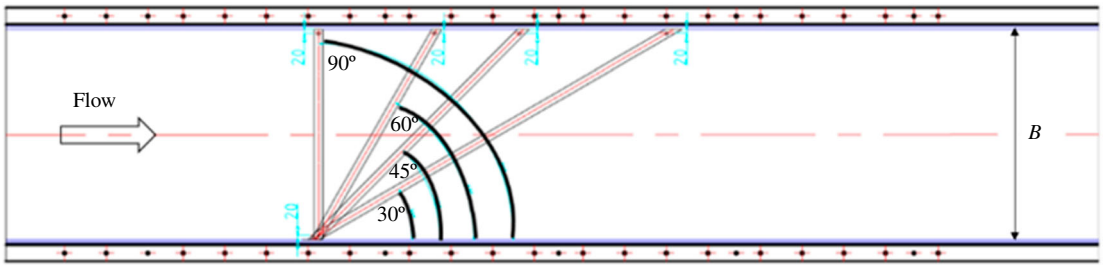

Figure 4 Top view of the four angles of orientation of the racks: 30°, 45°, 60° and 90°

the Microsonic type Mic = 35: IU:TC, with a display accuracy of 1%. They were placed at $x = -2.82$ m and $x = -1.27$ m upstream from the bar rack and at $x = 2.36$ m and $x = 3.26$ m downstream ($x = 0$ at the upstream extremity of the rack); two of them were designated to calculate the head losses (between the probe 1 and 2) and the others to verify and validate this calculation. This positioning aligns with the study of Raynal et al. (2013b). The sampling frequency was 200 Hz for 60 s of record. The water depth uncertainty was calculated with the index of Beaulieu et al. (2015) and varied between 1 and 3 mm.

The mean upstream (V_1) and downstream (V_2) velocities were calculated, giving the upstream (H_1) and downstream (H_2) water depths ($V = Q/B \times H$). With Bernoulli's equation, the head loss due to the rack (ΔH) is determined as:

$$\Delta H = (H_1 - H_2) + \left(\frac{{V_1}^2}{2g} - \frac{{V_2}^2}{2g}\right) + \Delta H_0 \qquad (1)$$

Herein ΔH_0 is equal to 1.47 mm for the flow rate of 0.5 $m^3\ s^{-1}$. The head loss coefficient is then calculated:

$$\zeta = \frac{\Delta H}{{V_1}^2/(2g)} \qquad (2)$$

Table 1 Tested racks and hydraulic parameters

Parameters	Values	Units
Bar thickness (b)	0.005	(m)
Bar depth (p)	0.040	(m)
Bar spacing (e)	0.005; 0.010; 0.020	(m)
Angle of orientation (α)	30; 45; 60; 90	(°)
Ratio (e/b)	1; 2; 4	(–)
Discharge (Q)	0.5	($m^3\ s^{-1}$)
Channel width (B)	1	(m)
Upstream water head (H_1)	0.7	(m)
Approach velocity (V_1)	0.72	($m\ s^{-1}$)
Reynolds number R_e	720,000	(–)
Bar Reynolds number R_{eb}	3600	(–)
Froude number F	0.275	(–)

In addition, the velocity profiles are characterized using an acoustic Doppler velocimeter (ADV; SonTek, San diego, California, USA) that measures the three components of the velocity with acoustic pulses reflected by the particles in the fluid, for a duration of acquisition of 1 min, a frequency of 50 Hz and a number of points equal to 3000, for each velocity component considering the signal-to-noise over time higher than 70%. Then, the points are filtered with an acceleration filter that calculates the acceleration of each particle of the fluid and considers only the maximal acceleration that is proportional to the gravity (g) or with the same order of magnitude (Goring & Nikora, 2002).

Two velocity profiles (6), upstream and downstream of the bar rack, were acquired for each configuration at mid-depth ($z = 350$ mm to the bottom of the channel, fixed for all profiles), on the x–y plane. The upstream profile was obtained 50 mm ahead of the rack front line. The transverse downstream profile was obtained 400 mm from the most downstream point of the bar rack, to characterize the velocity profile at the turbine intake. The profile mesh was done with a fixed step of 40 mm.

3 Head loss coefficients

3.1 *Experimental results*

The head loss coefficient has been represented according to the angle of orientation and the bar spacing for each bar shape (7). The maximum head loss coefficient, for spacing of PR bars equal to 5 mm, increases with the angle of orientation, from 1.4 for 30° to 4.7 for 90°. The minimum head loss coefficient, for spacing of PH bars equal to 20 mm, increases with the angle of orientation, from 0.3 for 30° to 0.5 for 90°. Perpendicular bar racks ($\alpha = 90°$) with PR bars and the lowest spacing ($e = 5$ mm) generates the highest head losses.

Figure 8 shows the evolution of the head loss coefficient according to the ratio between the bar spacing and the bar

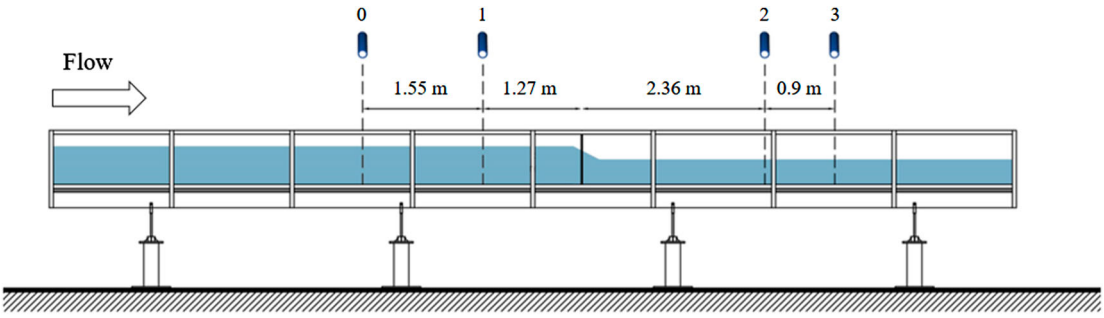

Figure 5 Side view of the channel showing the position of the water level gauges

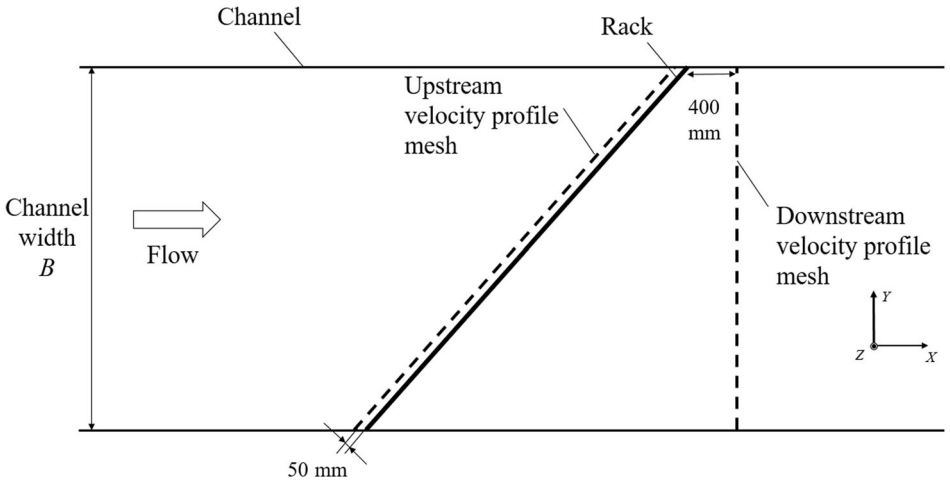

Figure 6 Top view of the channel and positioning of the velocity profile upstream and downstream of the racks

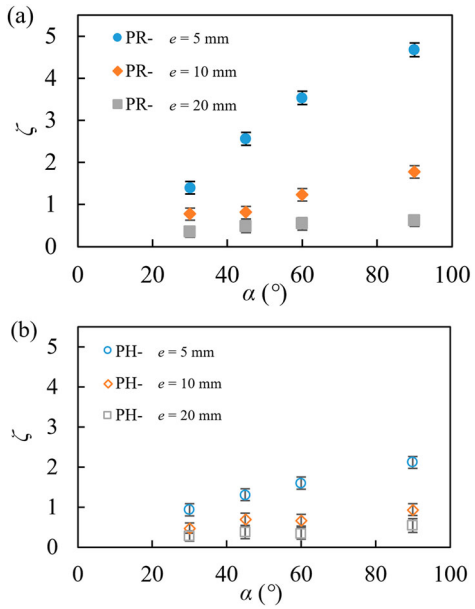

Figure 7 Comparison of measured head loss coefficients (a) for PR, (b) for PH, for three bar spacings (e) as a function of the rack angle (α)

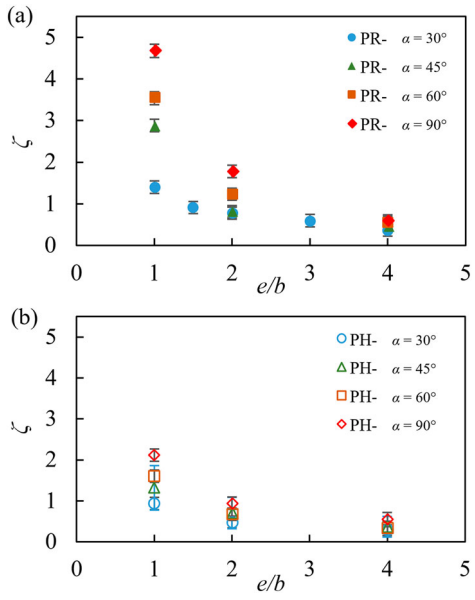

Figure 8 Comparison of measured head loss coefficients (a) for PR, (b) for PH and four angles of orientation (α), as a function of the ratio between bar spacing and bar thickness (e/b) (additional points were also measured and are presented concerning the 30° angle for ratios 1.5 and 3, to give more accuracy)

thickness for each bar shape, for $e/b = 1$, 2, 4. The head loss coefficient decreases with the e/b ratio. For an angle of 90°, the head loss coefficient is four times higher from a ratio of $e/b = 1$ to $e/b = 4$ (PH). Low bar spacing rack generates then higher head losses. The bar shape also influences the head losses, as PR tends to double the head loss coefficient compared to PH.

3.2 *Comparison with other measurements in the literature*

The comparison between recent measurements conducted on bar racks with horizontal bars is shown in 9. In the study of Böttcher et al. (2019), angled racks with horizontal cylindrical bars with

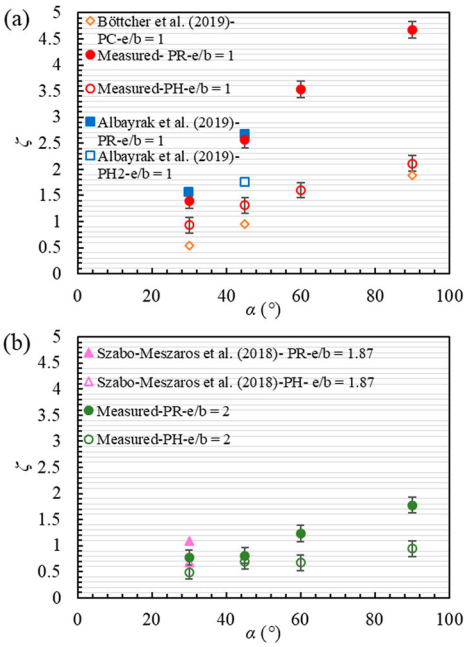

Figure 9 Comparison of measured head loss coefficients with literature data, as a function of the rack angle (α); (a) for $e/b = 1$ and (b) for $e/b = 2$ or 1.87; PC: cylindrical profile, PR: rectangular profile, PH: hydrodynamic profile (this study), PH2: hydrodynamic profile of Albayrak et al. (2020)

a diameter of 5 mm were tested for three angles (30°, 45° and 90°) and three bar spacings (5, 10 and 15 mm) ($e/b = 1$, 2, 3). Albayrak et al. (2020) also investigated bar racks with horizontal bars angled at 30° and 45°, with $e/b = 1$, 2, 3 and PH2 (which has a rounded front edge and a rectangular back edge) and PR bars. The study of Szabo-Meszaros et al. (2018) concerned several configurations of racks (angled with horizontal or vertical bars, positioned streamwise or perpendicular to the rack) for a single angle of 30°, a bar thickness of 8 mm and a bar spacing equal to 15 mm ($e/b = 1.87$).

The points show similar trends among the different set-ups, particularly when spacing ratio and bar shapes are identical. Nevertheless, the cylindrical profile seems to generate the lowest head loss coefficient. This is near to that generated by PH bars in the current studies. Despite this advantage, according to Böttcher et al. (2019) this type of shape may induce other issues like vortex-induced vibrations. For the angle of orientation of 30°, the head loss coefficients found in different articles are well superposed for the various bar shapes. The data are summarized in Table 2.

3.3 *Comparison between measurements and formulae in the literature*

The head loss coefficient has also been compared with formulae in the literature. Since the geometries of the horizontal angled and vertically inclined racks are identical, the formulae of Raynal et al. (2013a) and Meusburger (2002) with some adaptations are first investigated. Then, the formula developed for angled horizontal bar racks by Albayrak et al. (2020) is compared with them.

Table 2 Values of the head loss coefficients plotted in 9

Bar shape	α (°)	e/b	ζ Measured	ζ Böttcher et al. (2019)	ζ Szabo-Meszaros et al. (2018)	ζ Albayrak et al. (2020)
PR	30	1	1.40	–	–	1.56
PR	30	1.87	–	–	1.09	–
PR	30	2	0.77	–	–	–
PH	30	1	0.94	–	–	–
PC	30	1	–	0.53	–	–
PH	30	1.87	–	–	0.68	–
PH	30	2	0.48	–	–	–
PR	45	1	2.56	–	–	2.68
PH	45	1	1.31	–	–	–
PH2	45	1	–	–	–	1.76
PC	45	1	–	0.95	–	–
PH	45	2	0.70	–	–	–
PC	90	1	–	1.88	–	–
PH	90	2	0.94	–	–	–

The adapted formula of the head loss coefficient (ζ_R) modelled by Raynal et al. (2013a) is presented in Eq. (3):

$$\zeta_R = A_i \left(\frac{O_b}{1 - O_b} \right)^{1.65} \sin(\alpha)^2 + C \left(\frac{O_{sp,B}}{1 - O_{sp,B}} \right)^{0.77} \quad (3)$$

with:

$$O_b = \frac{N_{b,im} b}{H_1} \text{ and } O_{sp,B} = (1 - O_b) \frac{N_{sp} D_{sp}}{B}$$

where A_i is the bar shape coefficient, O_b the blockage ratio due to the bars, $O_{sp,B}$ the blockage ratio due to the vertical spacers relative to the channel cross-section, $N_{B,im}$ the number of immersed horizontal bars, b the bar thickness, H_1 the upstream water level, $C = 1.79$ is the bar shape coefficient of the spacers, N_{sp} the number of vertical spacer rows, D_{sp} the spacer diameter and B the channel width.

The adapted formula of the head loss coefficient (ζ_M) modelled by Meusburger (2002) is presented in Eq. (4):

$$\zeta_M = K_i \left(\frac{P}{1 - P} \right)^{1.5} \sin(\alpha) \quad (4)$$

with:

$$P = \frac{A_b + A_s}{A_t}$$

where K_i is the bar shape coefficient, P the blockage ratio, A_t the total rack area, A_b the area of the bars and A_s the area of the spacers.

The formula of the head loss coefficient (ζ_A) modelled by Albayrak et al. (2020) is presented in Eq. (5):

$$\zeta_A = K_i \left(\frac{P}{1 - P} \right)^{1.8} C_l C_\alpha \quad (5)$$

with:

$$P = \frac{A_b + A_s}{A_t}$$

where K_i is the bar shape coefficient, P the blockage ratio, C_l the bar head loss factor, C_α the angle of orientation head loss factor, A_t the total rack area, A_b the area of the bars and A_s the area of the spacers.

In 10, the plots represent the head loss coefficients for different angles of orientation with a rectangular bar profile for comparison between the experimental results and values computed by the formulae of Raynal et al. (2013a), Albayrak et al. (2020) and Meusburger (2002). The concordance between experimental values and the different formulae is given by the mean deviation between measured points and different formulae (Table 3). The formula of Raynal et al. (2013a), whose deviations vary from 0.05 to 0.10, provides the best approximation. These results show the applicability of this formula initially produced for inclined racks for the case of racks with horizontal bars. Also, the formula of Albayrak et al. (2020) overestimates the experimental values, managing a difference when the e/b ratio is small. This difference is due to the non-separation of the spacer term in this formula (modelled by Raynal et al., 2013a with $C(O_{sp,H}/1 - O_{sp,H})^{0.77}$). If in the formula of Albayrak et al. (2020) we set apart the spacer term and the bar term, and add the model of Raynal et al. (2013a) for the spacer term, we obtain the formula named by Albayrak et al. (2020) + spacer term. This formula of Albayrak et al. (2020) gives a satisfactory prediction for 30° and 45° angles, then differences increase for higher angles of orientation and low e/b ratios (but the formula of Albayrak et al., 2020 has not been validated for these configurations). The formula of Meusburger (2002) gives almost the same results as the one of Albayrak et al. (2020) for 30° and 45°.

3.4 *Comparison of head losses between several types of angled racks*

The head losses are compared for several types of angled bar racks. Figure 11 illustrates different configurations: angled racks with: horizontal bars (HB), vertical perpendicular bars (VPB), or vertical streamwise bars (VSB).

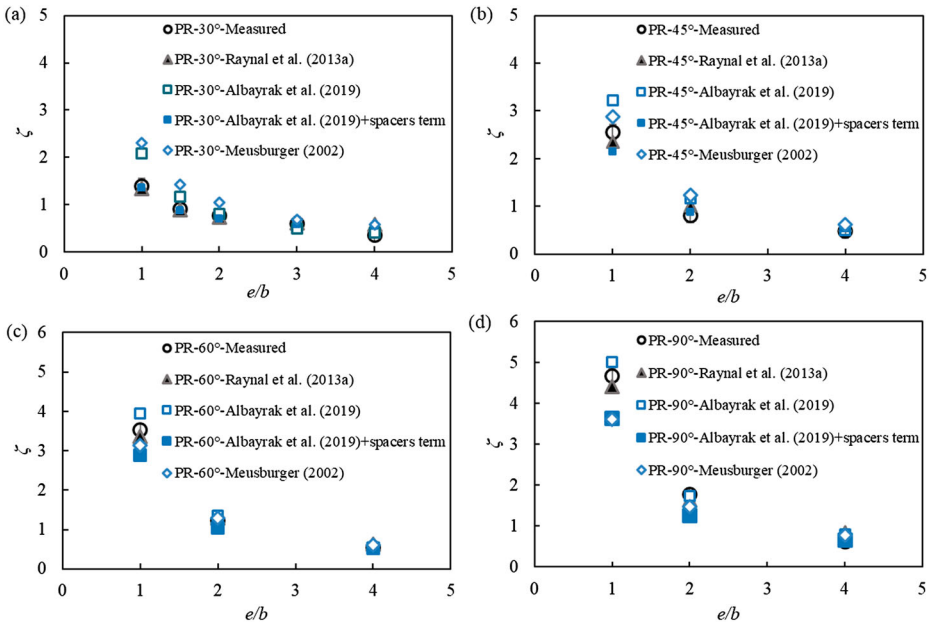

Figure 10 Comparison between measured head loss coefficients and head loss coefficients computed by the formulae of Raynal et al. (2013a), Albayrak et al. (2020) and Meusburger (2002), as a function of (e/b), for PR and different rack angles (α): (a) for 30°, (b) for 45°, (c) for 60° and (d) for 90°. (Additional points are presented concerning the 30° angle for ratios 1.5 and 3, to give more accuracy)

Table 3 Mean deviation between measured head loss coefficients and calculated head loss coefficients by the formulae, for the different rack angles (α)

α (°)	Raynal et al. (2013a)	Albayrak et al. (2020)	Albayrak et al. (2020) + spacers term	Meusburger (2002)
30	0.05	0.14	0.06	0.18
45	0.06	0.24	0.10	0.19
60	0.06	0.25	0.17	0.21
90	0.10	0.26	0.30	0.29

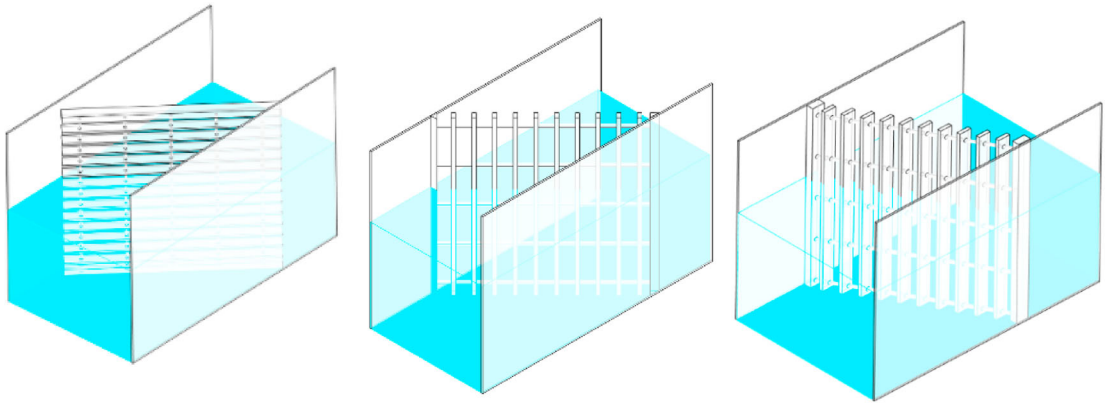

Figure 11 Angled bar racks with: horizontal bars (on the left), vertical perpendicular bars (in the centre), vertical streamwise bars (on the right)

Figure 12 shows a comparison of head loss coefficients between angled racks with vertical bars arranged perpendicularly to the rack axis computed with the formula of Raynal et al. (2013a) (Eq. 6), with streamwise bars computed with the formula of Raynal et al. (2014) (Eq. 7) and with horizontal bars computed with Eq. (3):

$$\zeta = K_i\left(\frac{O_g}{1-O_g}\right)^{1.6}\left(1+k_i\left(\frac{90^\circ-\alpha}{90^\circ}\right)^{2.35}\left(\frac{1-O_g}{O_g}\right)^{3}\right) \quad (6)$$

$$\zeta = K_i\left(\frac{O_g}{1-O_g}\right)^{1.6} \quad (7)$$

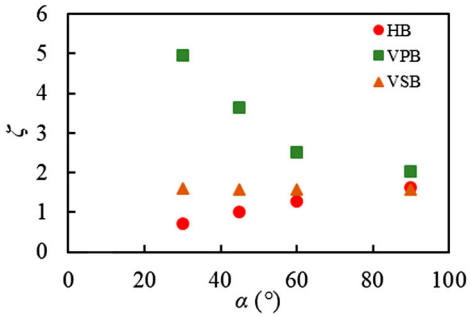

Figure 12 Comparison of head loss coefficient as a function of the rack angle (α) for VPB, VSB and HB with PR and $e/b = 2$

where K_i and k_i are coefficients depending on the bar shape, O_g the blockage ratio and α the angle of orientation.

Going from a perpendicular rack ($\alpha = 90°$) to a low angle of orientation, the head loss coefficients of angled racks with perpendicular vertical bars increase exponentially, coefficients of the racks with streamwise bars are constant and coefficients of the racks with horizontal bars decrease.

4 Velocity profiles

4.1 *Experimental results*

Two velocity profiles are recorded, 50 mm ahead of the rack front line and 400 mm downstream of the most downstream point of the rack. These are exposed in this section and discussed to verify the fish-friendly criteria upstream and to assess the flow homogeneity downstream of the bar racks. Figure 13 exposes the non-dimensional velocity profiles as a function of the Y coordinate (according to 6) for a rectangular bar profile, a bar spacing equal to 10 mm and the different angles of orientation. The four curves for the non-dimensional v_x/v_1 are similar, and values are constant at about 1, showing no effect of the angle of orientation and no heterogeneity over the channel width. Meanwhile, the non-dimensional normal velocity v_n/v_1 varies from about 0.5 for an angle of 30° and 1 for an angle of 90°, and is constant over channel width and in agreement with the theoretical value $v_n/v_1 = \sin(\alpha)$. Consequently, the ratio between the tangential and normal velocities v_t/v_n varies from approximately 0 for $\alpha = 90°$, to approximately 1 for $\alpha = 45°$ and 1.73 for $\alpha = 30°$, in agreement with the theoretical value $v_t/v_n = 1/\tan(\alpha)$.

Figure 14 exposes the non-dimensional tangential velocity profile v_t/v_1 for PH and PR bars. The profiles vary with the angle of orientation, approaching 0 for the 90° angle, compared to 0.8 for 30°, the lowest angle tested, without any effect of the bar profile. Values over the channel width are

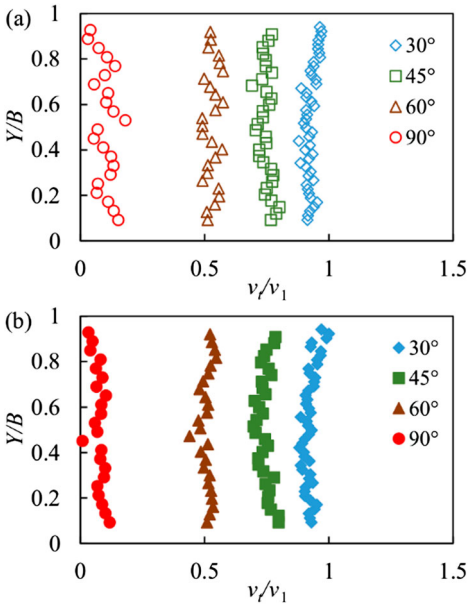

Figure 14 Comparison of the upstream non-dimensional tangential velocity profiles, (a) for PH and (b) for PR, for $e = 10$ mm and different rack angles (α)

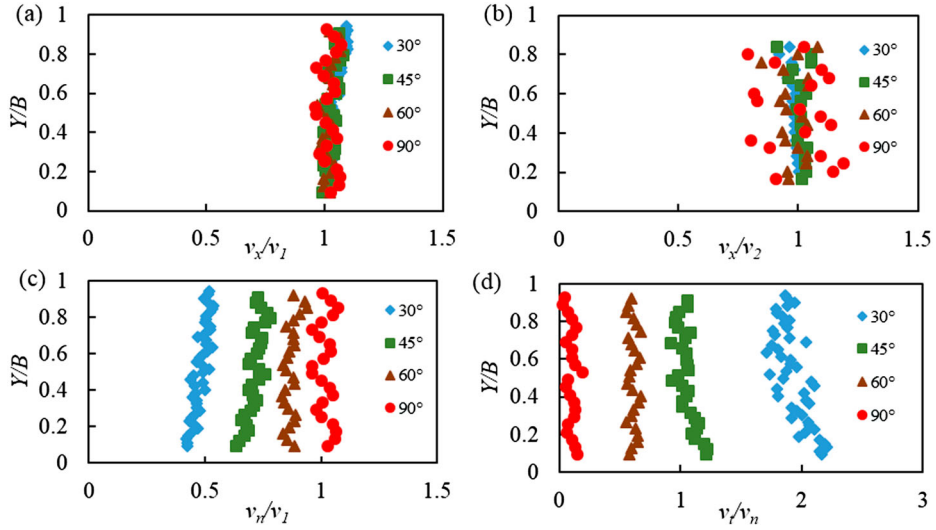

Figure 13 Comparison of the non-dimensional transverse velocity profiles for PR and $e = 10$ mm and different rack angles (α). (a) upstream streamwise velocity, (b) downstream streamwise velocity, (c) upstream normal velocity, (d) ratio between the tangential and normal velocities

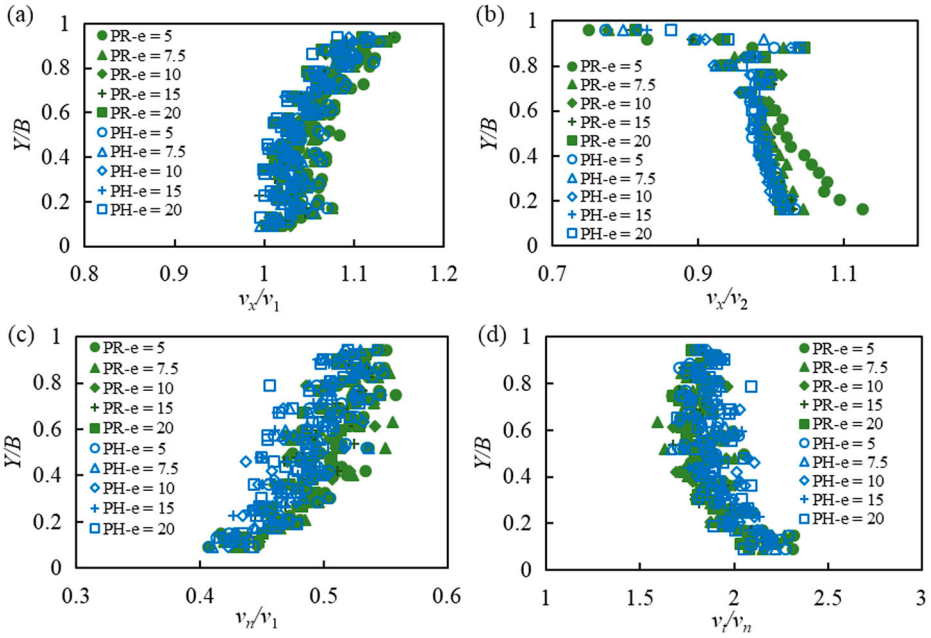

Figure 15 Non-dimensional velocity profiles as a function of the two bar shapes, and different bar spacings (e) for a rack angle $\alpha = 30°$. (a) Upstream streamwise velocity, (b) downstream streamwise velocity, (c) upstream normal velocity, (d) ratio between the tangential and normal velocities

nearly constant and are in agreement with the theoretical value $v_t/v_1 = \cos(\alpha)$.

Figure 15 shows non-dimensional velocity profiles for the 30° angle of orientation as a function of bar shape and bar spacing. The superposition of the curves is noticeable and proves the invariance of the velocity profile with the ratio between the bar spacing and the bar thickness. The non-dimensional v_x/v_1 velocity is influenced by the vertical rounded spacer bars, resulting in velocity deficits ahead of each support and an acceleration among the bars. The downstream velocity profile presents a deceleration at the end of the rack, located at $Y/B > 0.9$. This phenomenon is due to the blockage caused by the angle of orientation where the flow is constrained between the channel side and the end of the rack.

4.2 *Comparison of velocity profiles between several types of angled bar racks*

The velocity profiles of angled racks for different bar configurations, horizontal bars as measured in this study, vertical perpendicular bars of Raynal et al. (2013b) and the vertical streamwise bars of Raynal et al. (2014), are compared in order to assess the compliance with the biological criteria on flow field upstream the bar racks. The position of the two velocity profiles is the same for the three studies (50 mm ahead of the rack front line and 400 mm downstream of the rack, at mid-depth $z = 350$ mm from the bottom of the channel).

Figures 16 and 17 compare the profiles of non-dimensional normal and tangential velocities v_t/v_1 and v_n/v_1, and of the ratio

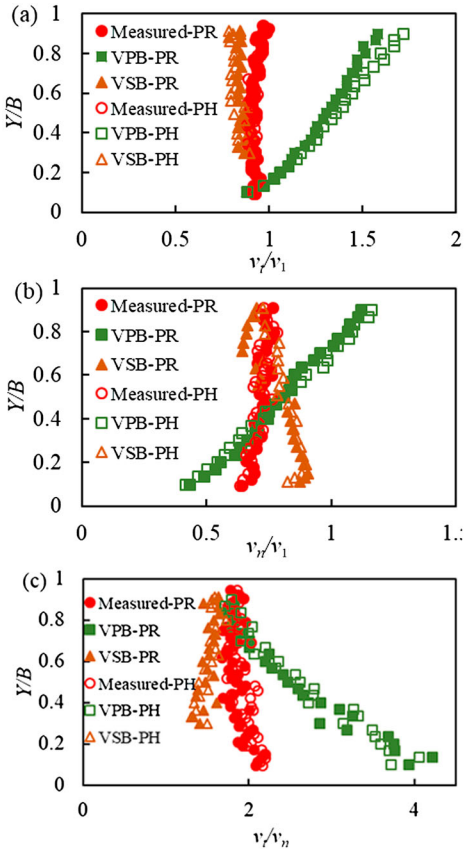

Figure 16 Comparison of non-dimensional velocity profiles for angled bar racks with VPB, VSB and HB, for a bar spacing $e = 10$ mm, the two bar shapes and a rack angle $\alpha = 30°$. (a) Upstream tangential velocity, (b) upstream normal velocity, (c) ratio between the tangential and normal velocities

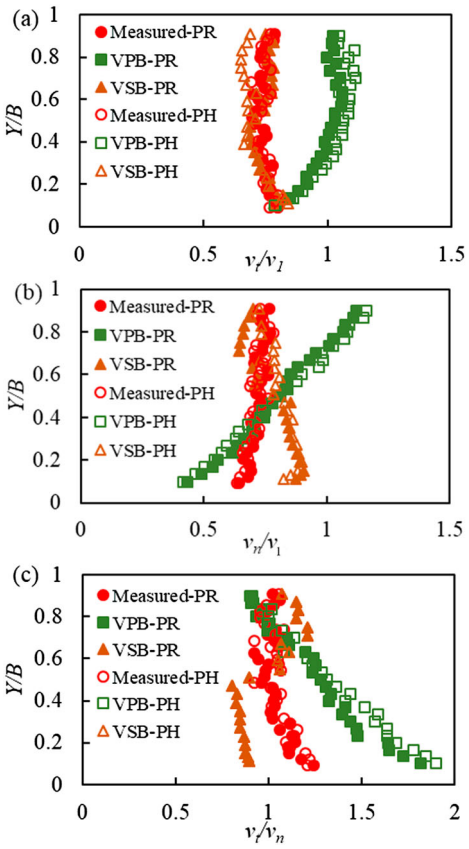

Figure 17 Comparison of non-dimensional velocity profiles for angled bar racks with VPB, VSB and HB, for a bar spacing $e = 10$ mm, the two bar shapes and a rack angle $\alpha = 45°$. (a) Upstream tangential velocity, (b) upstream normal velocity, (c) ratio between the tangential and normal velocities

v_t/v_n measured at the profile upstream from the rack, for an e/b ratio equal to 2, both bar shapes (PR and PH) and two angles (30° and 45°). The three velocity profiles along the rack with horizontal bars and along the rack with vertical streamwise bars are similar and nearly homogeneous over the channel width. In contrast, velocity profiles along the rack with vertical perpendicular bars show different trends, with an increase of v_t/v_1 and v_n/v_1 and a decrease of v_t/v_n from upstream to downstream. This is observed for both bar shapes and both angles.

Figure 18 compares the profiles of non-dimensional streamwise velocity on downstream velocity v_x/v_2, measured downstream of the racks, for an e/b ratio equal to 2, for PR bars and a 45° angle for the configurations of angled bar racks. The profile of VPB racks generates an asymmetric profile while the VSB and HB racks show homogeneous profiles over 80–90% of the channel width and reduced velocities in the 10–20% left along one bank (on the side of the upstream extremity of the rack for VSB and on the side of the downstream extremity of the rack for HB).

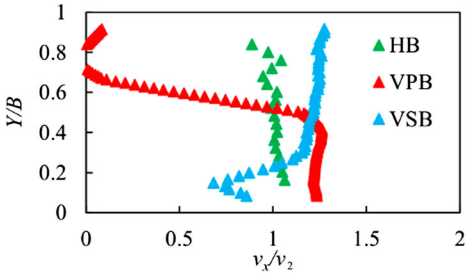

Figure 18 Comparison of non-dimensional downstream streamwise velocity profiles for angled bar racks with VPB, VSB and HB, for a bar spacing $e = 10$ mm, PR and a rack angle $\alpha = 45°$

4.3 *Compliance with biological criteria*

As the velocity profiles along angled racks with horizontal bars are in agreement with theoretical values, the compliance with the guidance criteria $v_t/v_n \geq 1$ is obtained for an angle of orientation $\alpha \leq 45°$. The maximum upstream approach velocity that satisfies the impingement criteria ($v_n \leq 0.5\,\mathrm{m\,s^{-1}}$) can be determined using:

$$v_{n,\max} = K \times \sin(\alpha) v_1$$
$$v_{n,\max} \leq 0.5\,\mathrm{m\,s^{-1}} \quad (8)$$

where $K = 1.2$ for bar racks with VSB; $K = 1.7$ for bar racks with VPB; and $K = 1.0$ for bar racks with HB. K is the ratio between the theoretical value of the normal velocity and the measured value of the normal velocity in the experiments obtained for VSB and VPB in the study of Raynal et al. (2014).

The resulting $K = 1.0$ is the criterion proposed for angled racks with horizontal bars. At $\alpha = 45°$, the maximal acceptable approach velocity v_1 is $0.7\,\mathrm{m\,s^{-1}}$. For higher values of approach velocity, the angle must be lowered to avoid impingement risks. For instance, for common values of velocity in water intakes, $v_1 = 0.8$ and $0.9\,\mathrm{m\,s^{-1}}$, the rack angles, with regard to the flow, must be $\alpha = 38°$ and 33°, respectively.

These criteria are close to, but less constraining than, those proposed for angled racks with vertical streamwise bars by Raynal et al. (2014). However, the compliance of biological criteria is significantly facilitated for these two types of modified angled racks, compared to "classical" angled racks with vertical perpendicular bars which have a much lower acceptable approach velocity for a given angle of orientation (Albayrak et al., 2018; Raynal et al., 2013b).

5 Conclusions

Angled trash racks with horizontal bars have been investigated for two main aspects: the head losses generated and the upstream and downstream velocity profiles for a total of 24 configurations, combining two bar shapes (PR and PH), three ratios between bar spacing and bar thickness ($e/b = 1$, 2 and 4) and four angles of orientation of the racks (30°, 45°, 60° and 90°).

The head loss coefficients increase with the blockage ratio of the rack and decrease for hydrodynamic bar profiles compared

to rectangular ones. Coefficients also decrease as the rack angle of orientation decreases, unlike angled racks with vertical bars. Our results are consistent with those of previous studies conducted on fewer configurations (Albayrak et al., 2020; Böttcher et al., 2019; Szabo-Meszaros et al., 2018). Furthermore, managing some adaptations, the formula proposed by Raynal et al. (2013a) for inclined bar racks is also adequate for angled bar racks with horizontal bars. A comparison of detailed independent data could improve the validity of this equation.

Velocity profiles show minor effect of the angle of orientation and no heterogeneity over channel width. Consequently, the normal and tangential components of the velocity along the rack are in agreement with their theoretical values given by angular decomposition. The compliance with the guidance criteria $v_t/v_n \geq 1$ is obtained for an angle of orientation $\alpha \leq 45°$. The upstream mean velocity for which the impingement criteria ($v_n \leq 0.5\,\mathrm{m\,s^{-1}}$) is satisfied depends on the angle ($v_1 = 0.7$, 0.8 and $0.9\,\mathrm{m\,s^{-1}}$ at $\alpha = 45°$, 38° and 33°, respectively). Concerning head losses and flow fields upstream and downstream of the rack, these results confirm that angled racks with horizontal bars are significantly less constraining than angled racks with vertical perpendicular bars, and measurably less constraining than angled racks with vertical streamwise bars. Angled racks with horizontal bars or streamwise bars may therefore improve fish protection for water intakes up to $100\,\mathrm{m^3\,s^{-1}}$ flow rate. However, bar racks with horizontal bars have already been implemented at several intakes of hydropower plants with discharge of up to $88\,\mathrm{m^3\,s^{-1}}$ and benefit from operational and biological feedback (Ebel, 2013), while to our knowledge there is still no full-scale installation of racks with streamwise bars.

Coupled with previous studies on inclined racks (Raynal et al., 2013a) and on angled racks with streamwise bars (Raynal et al., 2014), this study on angled bar racks with horizontal bars should help engineers to choose the best solution to design a fish-friendly intake at each site.

Funding

This project received funding from the European Union's Horizon 2020 research and innovation programme FITHydro (www.fithydro.eu), under grant agreement [No 727830].

Notation

A_i = bar shape coefficient (–)
b = bar thickness (m)
B = channel width (m)
L_g = trash rack width and bar length (m)
e = bar spacing (m)
g = gravitation acceleration ($\mathrm{m\,s^{-2}}$)
H_1, H_2 = upstream and downstream water depths respectively (m)
K_f = bar shape coefficient (–)
P, O_g = blockage ratio (–)
O_b = blockage ratio due to bars (–)
O_{sp} = blockage ratio of the spacing bars (–)
p = bar depth (m)
Q = flow rate ($\mathrm{m^3\,s^{-1}}$)
V_1, V_2 = upstream and downstream mean velocities respectively ($\mathrm{m\,s^{-1}}$)
v_t, v_n = components of the velocity tangential and normal to the rack face, respectively ($\mathrm{m\,s^{-1}}$)
α, β = angle of orientation or inclination respectively (°)
$\Delta H_0, \Delta H$ = head loss due to the channel and head loss due to the rack (m)
ζ = head loss coefficient (–)
C_l = head loss factor of bar depth (–)
C_α = head loss factor of the angle of orientation (–)

Abbreviation

HB = horizontal bars (–)
PR = rectangular bar shape (–)
PH = hydrodynamic bar shape (–)
PC = cylindrical bar shape (–)
PH2 = hydrodynamic bar shape of the study (Albayrak et al., 2020) (–)
VPB = vertical perpendicular bars (–)
VSB = vertical streamwise bars (–)

References

Albayrak, I., Kriewitz, C., Hager, W., & Boes, R. (2018). An experimental investigation on louvres and angled bar racks. *Journal of Hydraulic Research*, *56*(1), 59–75. doi:10.1080/00221686.2017.1289265

Albayrak, I., Maager, F., & Boes, R. (2020). An experimental investigation on fish guidance structures with horizontal bars. *Journal of Hydraulic Research*, *58*(3), 516–530. doi:10.1080/00221686.2019.1625818

Amaral, S., Winchell, F., McMahon, B., & Dixon, D. (2003). Evaluation of angled bar racks and louvers for guiding silver phase American eels. In D. Dixon (Ed.), *Proceedings of biology, management and protection of Catadromous Eels* (pp. 367–376). American Fisheries Society.

Beaulieu, C., Pineau, G., Ballu, A., David, L., & Calluaud, D. (2015, September 21–24). Démarche d'estimation des incertitudes de mesure dans un laboratoire de recherche: apport et perspectives – exemple d'un laboratoire de recherche en hydrologie des milieux aquatiques. In CIM (Ed.), *17th International Congress of Metrology*, Paris, France.

Böttcher, H., Gabl, R., & Aufleger, M. (2019). Experimental hydraulic investigation of angled fish protection systems—Comparison of circular bars and cables. *Water*, *11*(5), 1056. doi:10.3390/w11051056

CONSEIL, P. E. (2009, avril 23). DIRECTIVE 2009/28/CE. Journal officiel de l'Union européenne.

Courret, D., & Larinier, M. (2008). *Guide pour la conception de prises d'eau "ichtyocompatibles" pour les petites centrales hydroélectriques [Guide for the design of fish-friendly intakes for small hydropower plants]*. Report No RAPPORT GHAAPPE RA.80.40, Agence de l'Environnement et de la Maitrise de l'Energie (ADEME), France. http://oai.afbiodiversite.fr/cindocoai/download/PUBLI/152/1/2008_027.pdf 2258Ko (in French).

Courret, D., Larinier, M., David, L., & Chatellier, L. (2015, June 24). Development of criteria for the design and dimensioning of fish-friendly intakes for small hydropower plant. *International Conference on Engineering and Eco-hydrology for Fish Passage*, The Netherlands. Groningen. https://scholarworks.umass.edu/fishpassage_conference/2015/June24/16/

Ebel, G. (2013). *Fischschutz und Fischabstieg an Wasserkraftanlagen. Handbuch Rechen- und Bypasssysteme. Ingenieurbiologische Grundlagen, Modellierung und Prognose, Bemessung und Gestaltung* [Fish protection and downstream passage at hydro power stations. Handbook of bar rack and bypass systems. Bioengineering principles, modelling and prediction, dimensioning and design]. Mitteilungen aus dem Büro für Gewässerökologie und Fischereibiologie. Saale.

Electric Power Research Institute (EPRI). (2001). *Review and documentation of research and technologies on passage and protection of downstream migrating catadromous eels at hydroelectric facilities*. Report EPRI. https://www.epri.com/research/products/1000730.

Godde, D. (1994). *Experimentelle Untersuchung zur Anströmung von Rohrturbinen: Ein Beitrag zur Optimierung des Turbineneinlaufs [Experimental investigation of bulb turbine admission flow: Contribution to the intake optimization]*. Munich: Obernach Research Institute, and Chair of Hydraulic and Water Resources Engineering TU Munich.

Goring, D., & Nikora, V. (2002). Despiking acoustic doppler velocimeter data. *Journal of Hydraulic Engineering*, *128*(1), 117–126. doi:10.1061/(ASCE)0733-9429(2002)128:1(117)

Huusko, R., Hyvarinen, P., Jaukkuri, M., Maki-Petays, A., Orell, P., & Erkinaro, J. (2018). Survival and migration speed of radio-tagged Atlantic salmon (Salmo salar) smolts in two large rivers: one without and one with dams. *Canadian Journal of Fisheries and Aquatic Sciences*, *75*(8), 1177–1184. doi:10.1139/cjfas-2017-0134

IEA, I. E. (2017). *Key world energy statics*.

Larinier, M., & Travade, F. (2002). Downstream migration: Problems and facilities. *Bulletin Français de la Pêche et de la Pisciculture*, *364*, 181–207. doi:10.1051/kmae/2002102

Meusburger, H. (2002). Energieverluste an Einlaufrechen Von Flusskraftwerken [Head losses at intakes of run-of-river hydropower plants]. In H.-E. Minor (Ed.), *VAW Mitteilung Nr. 179* (pp. 1–272). Laboratory of Hydraulics, Hydrology and Glaciology (VAW), ETH Zurich, CH (in German).

Montén, E. (1985). *Fish and turbines: Fish injuries during passage through power station turbines*. Norstedts Tryckeri. Vattenfall, 111p.

Raynal, S., Chatellier, L., Courret, D., Larinier, M., & David, L. (2014). Streamwise bars in fish-friendly angled trashracks. *Journal of Hydraulic Research*, *52*(3), 426–431. doi:10.1080/00221686.2013.879540

Raynal, S., Courret, D., Chatellier, L., Larinier, M., & David, L. (2013a). An experimental study on fish-friendly trashracks – Part 1. Inclined trashracks. *Journal of Hydraulic Research*, *51*(1), 56–66. doi:10.1080/00221686.2012.753646

Raynal, S., Courret, D., Chatellier, L., Larinier, M., & David, L. (2013b). An experimental study on fish-friendly trashracks – Part 2. Angled trashracks. *Journal of Hydraulic Research*, *51*(1), 67–75. doi:10.1080/00221686.2012.753647

Szabo-Meszaros, M., Ushanth Navaratnam, C., Aberle, J. T., Silva, A., Forseth, T., & Calles, O. (2018). Experimental hydraulics on fish-friendly trash-racks: an ecological approach. *Ecological Engineering*, *113*, 11–20. doi:10.1016/j.ecoleng.2017.12.032

Verbiest, H., Breukelaar, A., Ovidio, M., Philippart, J.-C., & Belpaire, C. (2012). Escapement success and patterns of downstream migration of female silver eel Anguilla anguilla in the River Meuse. *Ecology of Freshwater Fish*, *21*(3), 395–403.